

## INTRODUCTION

### 1.1 PEROVSKITE OXIDES

The natural occurring perovskite calcite ( $\text{CaTiO}_3$ ) was discovered by German Chemist and Mineralogist Gustav Rose in 1839, which further known as Perovskite in the name of Lev Alexeievitch Perovsky, a Russian Military official. Although the term ‘perovskite’ was initially reserved for  $\text{CaTiO}_3$ , it was later applied to synthetic compounds with a similar stoichiometry and crystal structure to the minerals [1]. Goldschmidt extensively studied the first synthetic perovskites and pioneered many principles that remain applicable to the structure even today [2].

Perovskite oxides having the general formula  $\text{ABO}_3$  where A and B are cations and O is an anion. The valency of cation A and B varies from  $1^+$ ,  $2^+$ ,  $3^+$  and  $3^+$ ,  $4^+$ ,  $5^+$  in such a way that its total charge becomes six respectively in order to compensate the overall charge on perovskite. These perovskite oxides were similar to naturally occurring mineral  $\text{CaTiO}_3$ .

The structure of these materials varies and characterized by an octahedron of oxygen anions surrounding the transition metal cation that collectively site inside of a simple cubic cage of cations. Generally, in the perovskite A-site is 12-fold coordination and the B- site is 6-fold coordination, with both cations sharing their coordination with the oxygen anions as shown in Figure 1.1. Since in most of the perovskite oxides the interesting electronic interactions take place between the oxygen octahedral cages, it may be more useful to think of the perovskite structure as a network of corner-sharing octahedral complexes.

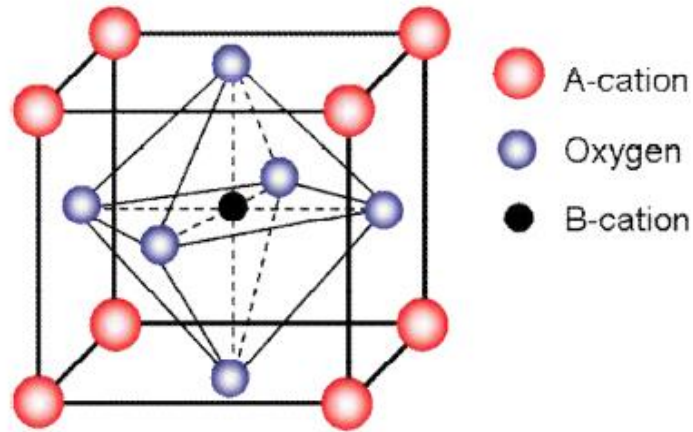


**Figure 1.1** A unit cell of  $ABO_3$  type cubic perovskite oxide structure

The ideal perovskite structure has a cubic unit cell having space group  $Pm\bar{3}m$  contains one formula unit. Due to distortion among the atoms the perovskite exhibited different structures depends on the value of the tolerance factor ( $t$ ). The tolerance factor for the ideal perovskite structure is defined through mathematical relation given by:

$$t = \frac{r_A + r_O}{\sqrt{2}(r_B + r_O)} \quad (1.1)$$

Where  $r_A$  and  $r_B$  are the ionic radius of cations A and B respectively whereas  $r_O$  is the ionic radius of the anion O. The numerical values of  $t$  depend on the ionic radii and give a rough estimation for the determination of crystal structure. Depending on the values of tolerance factor various crystal structure are possible, a list of tolerance factors ( $t$ ) with the existence of their crystal structure were tabulated in Table 1.1.

**Table 1.1** Tolerance factor of different crystal structure

Goldschmidt tolerance factor (t)	Structure	Explanation	Example
>1.0	Hexagonal or Tetragonal	A ion too big or B ion too small.	BaNiO <sub>3</sub> [3]
0.90-1.00	Cubic	A and B ions have ideal size.	SrTiO <sub>3</sub> [3] BaTiO <sub>3</sub> [4]
0.71 - 0.90	Orthorhombic/Rhomb ohedral	A ions too small to fit into B ion interstices.	GdFeO <sub>3</sub> (Orthorhombic) [3] CaTiO <sub>3</sub> (Orthorhombic) [1,3]
<0.71	Different structures	A ions and B have similar ionic radii.	Ilmenite, FeTiO <sub>3</sub> (Trigonal) [5]

## 1.2 ALKALINE EARTH TITANATE PEROVSKITES

Among the various studied alkaline earth titanates, the Calcium titanate is existed in nature and exhibited as a paraelectric material with cubic structure [6]. It has been reported that the symmetry of calcium titanate at room temperature is orthorhombic and shows a structural transition at 600<sup>0</sup>C to tetragonal and further transform to cubic at 1000<sup>0</sup>C.

In commercial multilayer ceramic capacitors (MLCs), perovskite structure titanates are frequently used as high permittivity dielectrics. Alkaline earth titanate such as CaTiO<sub>3</sub>, SrTiO<sub>3</sub>, and BaTiO<sub>3</sub>, etc. has been studied extensively for technological applications as well as in primary science due to its impressive electronic properties, chemical stability and structural behavior [7]. The SrTiO<sub>3</sub> was used as substrates for the growth of heteroepitaxial film for high T<sub>c</sub>

superconductors [8], in multi-layer capacitors [9] and Dynamic random access memory (DRAM) devices, etc.

Barium titanate ( $\text{BaTiO}_3$ ) was synthesized to become the first and the most widely studied ceramic material, due to its excellent dielectric, ferroelectric and piezoelectric properties [10]. The high dielectric constant of  $\text{BaTiO}_3$  ceramics results due to transition in their crystal structure. The various structural phase transitions in the  $\text{BaTiO}_3$  system was shown in Figure 1.2. The tetragonal polymorph is the most widely used because of its excellent ferroelectric, piezoelectric, and thermoelectric properties [11]. The temperature was a substantial factor which affects the crystal structure and polarization characteristics of  $\text{BaTiO}_3$ . The first structural transition takes place at  $120^\circ\text{C}$ ), from tetragonal to cubic and remains stable up to  $1400^\circ\text{C}$ . The  $\text{BaTiO}_3$  was a spontaneous random polarization at room temperature due to the presence of non-centrosymmetry in the center of oxygen octahedron. As temperature increases the thermal vibration is high and enough to results in the random orientation of the titanium ions in its octahedral interstitial position in  $\text{BaTiO}_3$ . The shift in the position of  $\text{Ti}^{4+}$  ion resulting increase in polarization when an electric field is applied, but it returns to its stable central position as soon as the field is removed. Thus, there is no retained polarization, no hysteresis loop, and no ferroelectric behavior. As the temperature of  $\text{BaTiO}_3$  is lowered slightly below  $120^\circ\text{C}$  (Curie temperature), a displacive transformation occurs in which the structure of the  $\text{BaTiO}_3$  changes from cubic to tetragonal. One crystallographic axis increases in length (unit cell goes from 4.010 to 4.022 Å) and the other two decrease in length (from 4.010 to 4.004 Å). The  $\text{Ti}^{4+}$  ion moves off-center toward one of the two oxygen ions of the long axis, resulting in a spontaneous increase in positive charge in this direction. The dielectric properties of  $\text{BaTiO}_3$  were found to be dependent on the grain size and temperature. At the Curie point, large-grained  $\text{BaTiO}_3$  ( $\geq 10 \mu\text{m}$ )

has a high dielectric constant because of the formation of multiple domains in a single grain, the motion of whose walls increases the dielectric constant at Curie point. For a BaTiO<sub>3</sub> with fine-grains (~1μm), a single domain forms inside each grain. The movement of domain walls is restricted by the grain boundaries, thus leading to a low dielectric constant at the Curie point compared to coarse-grained BaTiO<sub>3</sub>. At room temperature, the dielectric constant of coarse-grained BaTiO<sub>3</sub> ceramics was found to be in the range of 1500-2000. On the other hand, fine-grained BaTiO<sub>3</sub> exhibits a room temperature dielectric constant between 3500-6000. This is because the internal stresses in fine-grained BaTiO<sub>3</sub> are higher than in the coarse-grained material, which leads to a higher permittivity at room temperature [12].

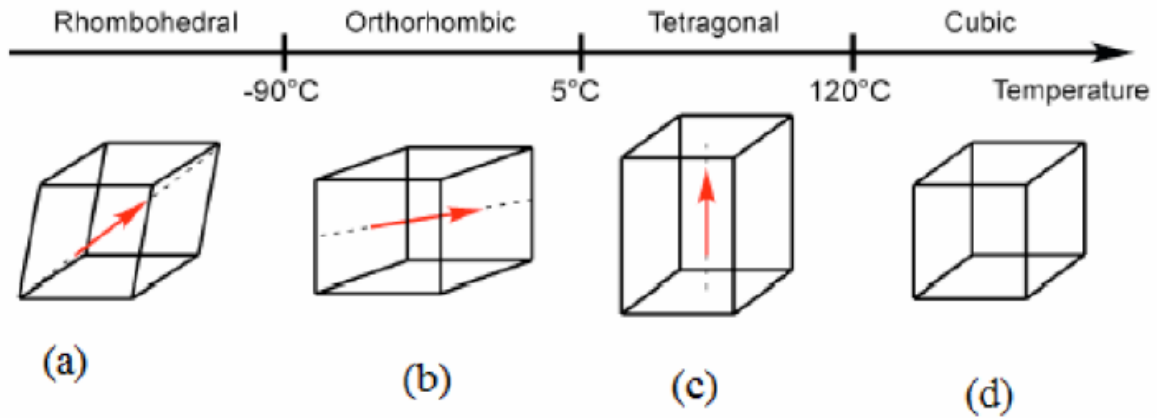


**Figure 1.2** Phase transition of BaTiO<sub>3</sub> system

### 1.3 ALKALINE EARTH STANNATE PEROVSKITES

Alkaline earth stannates (MSnO<sub>3</sub>: Ca, Sr, Ba) showing exciting properties similar to their titanates but Stannates received much attention by Wainer in 1946 when disclosed it as ceramic dielectric bodies comprised of alkaline-earth stannates and alkaline earth titanates in a series of patents. Perovskite-type alkaline earth metal stannates have received increasing attention due to

their extensive applications in ceramic dielectric bodies [13, 14], gas sensors [15-17], anode materials for lithium-ion batteries [18-22] and photocatalysts [23-29]. Thangadurai et al. [30] and Mishra et al. [31] reported that Fe substituted  $\text{SrSnO}_3$  compounds exhibit both ionic and electronic conductivity and may be vital material to be employed in solid oxide fuel cells (SOFC) application. The rare earth doped  $\text{SrSnO}_3$  were investigated for the humidity sensitivity and optical device application by the selection of appropriate dopant into the host [32]. Among various studied stannates, the barium stannates were extensively studied their intrinsic properties and tailoring of their electrical, magnetic and optical properties based on the modification of crystal structure, grains, etc. It has been reported that sensors based on  $\text{BaSnO}_3$  are sensitive to a variety of gasses, e.g.,  $\text{CO}$ ,  $\text{O}_2$ ,  $\text{C}_2\text{H}_5\text{OH}$ ,  $\text{CH}_3\text{SH}$ , LPG, and  $\text{NO}_x$  [33, 34]. S. Upadhyay et al. studied the detailed dielectric and electrical properties of  $\text{BaSnO}_3$  for the application in humidity sensitivity and electrolyte for an intermediate temperature solid oxide fuel cell (IT-SOFCs) by the selection of appropriate dopant into the host via doping and co-doping [35]. Furthermore,  $\text{BaSnO}_3$ - based systems are found to be good candidates for photocatalytic applications [36, 37]. Mizoguchiet *et al.* [38] reported that  $\text{BaSnO}_3$  exhibits strong near-infrared luminescence at room temperature.  $\text{BaSnO}_3$  has been developed as electrode application in the dye-sensitized solar cell [39, 40]. Barium stannate based systems  $\text{BaSn}_{1-x}\text{M}_x\text{O}_{3-\delta}$  (where  $\text{M} = \text{Fe}, \text{Sc}, \text{In}, \text{Y}, \text{Gd}, \text{Sm}, \text{Nd}$ , and  $\text{La}$ ) also have been proposed as proton conductors with potential applications in the fuel cell [41, 42]. Recently thin films of  $\text{BaSnO}_3$ -based oxides have attracted much attention as novel transparent conducting oxides (TCO) material due to their excellent physical properties among the perovskite oxides [43–45]. Transition metal such as  $\text{Fe}, \text{Co}, \text{Ni}$ , etc. doped  $\text{BaSnO}_3$  was widely investigated for the magnetic memory devices and spintronics application [46]. These types of materials were working as dilute magnetic semiconductor because of the lower doping

concentration of transition metals tailor the magnetic properties of host for the different applications in magnetism.

## **1.4 SOLID SOLUTION OF PEROVSKITES**

The perovskite oxides in undoped form have only limited applications while the compositional modification in perovskite oxides was useful in tailoring their properties. Depending on the valence of the dopant ion following are different types of compositional modifications processes:

- (i) Isovalent substitutions
- (ii) Hetro-valent substitutions
- (iii) Valence compensated substitutions

### **1.4.1 Isovalent Substitutions**

Isovalent substitution is of the type  $AA'BO_3$  or  $ABB'O_3$  where A and A' or B and B' ions have the same valency. For example;  $Ca^{2+}$ ,  $Sr^{2+}$  on  $Ba^{2+}$  site and  $Zr^{4+}$ ,  $Sn^{4+}$  on  $Ti^{4+}$  site in  $BaTiO_3$ .

### **1.4.2 Hetro -Valent Substitutions**

In this category of substitutions, the substituents ion which is being substituted has different valences than host ion. These substitutions also may be on either A or B sites. Hetro-valent substitutions are of two types:

i. Acceptor substitutions: An acceptor ion has lower valency than that of the host ion it replaces, and the resulting negatively charged impurity center can be compensated by oxygen vacancy or donor impurity of holes, e.g., substitution of n  $Na^+$  on  $Ba^{+2}$ ;  $Co^{+3}$  on  $Ti^{+4}$  sites in  $BaTiO_3$

ii. Donor substitution: In this case, the substituent impurity ion has higher valency than that

of host ion A or B sites. The impurity thus bears a sufficient positive charge, e.g.,  $Y^{+3}$  on  $Ba^{+2}$  and  $Nb^{+5}$  on  $Ti^{+4}$  site in barium titanate separately. Charge compensation, in this case, is achieved either through electrons or cations vacancies on A or B sub lattices [47].

### 1.4.3 Valence Compensated Substitutions

In this case, simultaneous substitutions of a combination of ions at A and B sublattice sites are such that total electrical charge neutrality in the crystal is maintained internally. Simultaneous valence compensated substitutions are of two type ( a) concurrent substitution of isovalent ions A and b sub lattices sites e.g.  $Pb_{1-x}Ba_xTi_{1-x}Sn_xO_3$  and (b) simultaneous substitution of hetrovalent ions on A and B sub lattice sites so that the charge balance is maintained internally without requiring the charge in the oxidation state of an ion or creation vacancies in A, B or O sub lattices such as  $M_{1-x}La_xTi_{1-x}M'_xO_3$  ( $M=Ca^{+2}$ ,  $Sr^{+2}$ ,  $Ba^{+2}$  or  $Pb^{+2}$  and  $M' = Co^{+3}$ ,  $Ni^{+3}$  or  $Fe^{+3}$ , etc.) [48-51]. Such solid solutions are known as valence compensated solid solution (VCSS).

## 1.5 SOLID SOLUTION OF $BaTiO_3$ - $BaSnO_3$

In this section we give a brief overview of some solid solutions with isovalent substitution in the B position of the perovskite cell (position of  $Ti^{+4}$ ), focusing on the studied system in the present work. Another system which has a diffuse phase transition is the solid solution composed by the ferroelectric  $BaTiO_3$  and the non-ferroelectric  $BaSnO_3$  on high Sn additions [52]. The substitution of  $Sn^{+4}$  on the B position of the perovskite cell produces changes to the Curie temperature and maximum dielectric values similar to those characteristic to other solid solutions based on  $BaTiO_3$ . The  $Ba(Ti_{1-x}Sn_x)O_3$  has drawn the attention due to the different abnormalities of the dielectric properties and the presented strong dielectric nonlinearity [53]. A phase diagram for this system was proposed by X. Wei and other authors have studied different aspects of some functional properties of this system [54, 55]. In that diagram, the compositions between (0.10,



0.15) at temperatures around room temperature, there seems to be a superposition of several structural phases (rhombohedral, tetragonal and cubic). In contrast, S. Markovic [56] found a continuous reduction of the tetragonality degree with increasing Sn concentration, reaching a value of 1 (specific cubic structure) for Sn concentration  $x = 0.12$ . Although there are various scientific articles that have as a topic the BTS ceramic system, the phase transitions sequence induced by the addition of Sn

is not yet fully understood and there is still missing a detailed analysis of the functional properties in connection with the composition, the microstructure and the phase symmetry. The present study focuses on the investigation of ferroelectric ceramic systems with the composition  $\text{Ba}(\text{Ti}_{1-x}\text{Sn}_x)\text{O}_3$ , the identifying superposition of phases, the relaxor state description and how these characteristics are reflected in the dielectric properties under weak field and intense field (dielectric nonlinearity), and the detection by combined experiments of multiple polar contributions to macroscopic properties. Therefore, the investigation of this area of composition and understand how to control at the micro level the system characteristics and therefore macroscopic properties by adjusting preparation conditions.

## **1.6 FERROELECTRIC MATERIALS**

There has been continuous interest in the fabrication of new ferroelectric materials since the discovery of ferroelectricity in a single crystal of Rochelle salt [57] and its subsequent extension into the domain of polycrystalline ceramics of barium titanate during the mid-1940s [58]. The development of new ceramic processing and thin film technology tin-based materials having a wide range of industrial and commercial applications. Application of these materials includes high dielectric constant capacitors piezoelectric sonar and ultrasonic transducer, radio and

communication filters, pyroelectric security surveillance devices, medical diagnostic transducer and different types of sensors [59].

Crystals can be divided into 32 - point groups according to their symmetry with respect to the point of these 32-points groups 21 are noncentrosymmetry and 20 of these are piezoelectric. Among these 20, ten have a unique polar axis and possess spontaneous polarization (which is in general temperature dependent), are called pyroelectric. Similar to pyroelectric materials, ferroelectric materials maintains spontaneous polarization, but the magnitude and the direction of the polarization can be reversed by external electric field. Ferroelectric materials are characterized by the following specific properties:

- 1) It has a spontaneous polarization domain structure under a certain temperature. Spontaneous polarization can be reversed by the action of an external field between values of saturation polarization ( $\pm P_S$ ), a phenomenon accompanied by the polarization hysteresis and remanence.
- 2) During the transition from the polar state (ferroelectric) to the non-polar one,(paraelectric) ferroelectrics shows a transition phase that can be of order I or II. The paraelectric phase always has a higher symmetry than the ferroelectric one.
- 3) Temperature dependence of electrical, mechanical, optical, caloric quantities and structural parameters present abnormalities on the phase transition

Ferroelectrics are dielectrics for which the relationship between polarization and an electric field is nonlinear and with hysteresis effects, i.e., the polarization values on increase/decrease the applied field may be different.

Ferroelectric crystals contain a region with uniform polarization called ferroelectric domains. Within domains, all the electric dipoles are aligned in the same directions. The domains are

separated from each other by an interface called domain walls. The polarization of domains can be reversed by applying a strong electric field and is known as domain switching.

There are three types of ferroelectric materials

- 1) Normal ferroelectric
- 2) Diffused phase transition ferroelectric
- 3) Relaxor ferroelectric

### 1.6.1 Normal Ferroelectric

One distinctive characteristic of ferroelectric is the hysteresis loop in the polarization versus electric field curve as shown Figure 1.3.

When the electric field is removed at the maximum point of saturation  $P_s$ , a remanent polarization  $P_r$  remains due to the coupling between the dipoles, which means the material is permanently polarized.

When a field is applied in the opposite direction, the polarization will be reversed. A coercive field  $E_c$  must be applied to remove the polarization and randomize the dipoles. If the reverse field is increased further, saturation occurs with the opposite polarization.

When the temperature increases, a ferroelectric crystal undergoes a structural phase transition from a ferroelectric phase to a paraelectric phase. The temperature at which the spontaneous polarization disappears is called the Curie temperature,  $T_c$

In paraelectric phase, the dielectric constant obeys Curie-Weiss law.

$$\text{Normal ferroelectric: } \frac{1}{\epsilon} = \frac{T - T_c}{C} \quad (1.2)$$

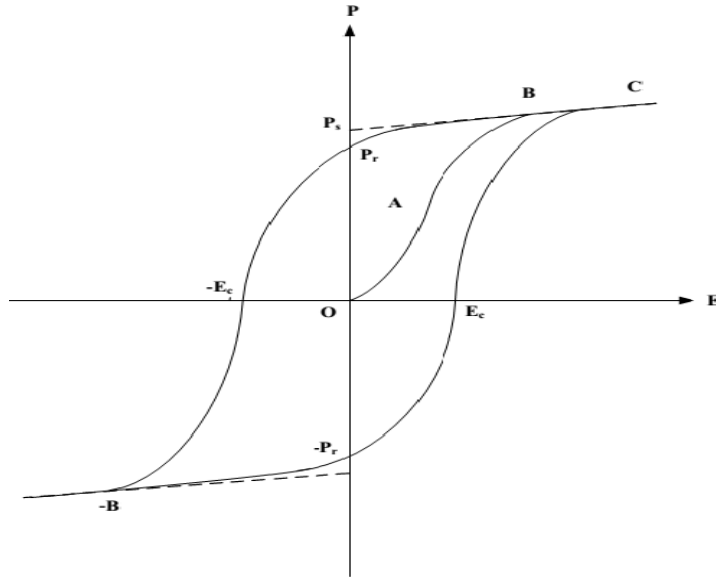


**Figure 1.3** Hysteresis loop in the polarization versus electric field curve

### 1.6.2 Diffused Phase Transition

The capacitance-temperature curves of some ferroelectrics show broad maxima and a large deviation from the Curie-Weiss law. These characteristics are explained on the basis of diffuse phase transitions. Ferroelectric to paraelectric phase transition which extends over a temperature interval due to the coexistence of two or more phases within a range of temperatures is known for isovalent as well as isovalent-substituted  $\text{BaTiO}_3$  solid solutions.  $\text{Ba}(\text{Ti}, \text{Sn})\text{O}_3$ ,  $\text{Ba}(\text{Nb}_{1.5}\text{Zr}_{0.25})\text{O}_{5.25}$ ,  $\text{Ba}(\text{Ti}, \text{Zr})\text{O}_3$ ,  $(\text{Ba}, \text{Sr})\text{TiO}_3$  and  $(\text{Ba}, \text{Nd})\text{TiO}_3$  are reported to show diffuse phase transition behaviour [60-62]. The nature of DPT cannot be described by the classical theory of ferroelectric transition. Its origin is not clear and is considered to be associated with either compositional or thermal or inter-granular strain [63-65]. Point defects arising from the inherent nonstoichiometry can also induce DPT behavior [66]. Generally, materials showing DPT behavior are considered to contain polarized micro-regions called Känzig regions, all having somewhat different phase transition temperatures [67]. These small differences may be due to mechanical stress distribution in the material or due to the variations in chemical

composition caused during sintering. Implied in this concept is the increased stress in microstructure during the cubic to tetragonal transition, which is largely compensated by ferroelectric domains. For ceramics of smaller grain size (less than a few microns), this compensation is incomplete and is said to be the major reason for the observed distribution of  $T_c$ . The contribution from chemical inhomogeneity (e.g., resulting from differences in the Ti/Sn ratio) to the distribution of  $T_c$  can be small. The spread of  $T_c$  values arises from the decrease in the heat of transformation with an increase in chemical inhomogeneity. Since the enthalpy change tends to zero, the free energy change around  $T_c$  should be very small.

Some characteristics of the DPT are: (a) broadened maxima in the permittivity- temperature curve, (b) gradual decrease of spontaneous and remnant polarizations with rising temperature, (c) transition temperatures obtained by different techniques which do not coincide, (d) relaxation character of the dielectric properties in transition region, and (e) no Curie-Weiss behavior in certain temperature intervals above the transition temperature.

### **1.6.3 Relaxor Ferroelectric**

In the 1950's, Smolenski et al. first discovered relaxor ferroelectrics. The difference between a normal ferroelectric and a relaxor was discussed by the behavior around the Curie point which is illustrated in Figure 1.4. Considering the dielectric response of normal ferroelectric, when the temperature is above Curie temperature,  $T_c$ , the dielectric constant can be obtained by Curie-Weiss law which is shown in Equation. (1.2). Normal ferroelectric exhibits the sharp first order dielectric transition peak as a function of temperature. In relaxor ferroelectrics exhibit a broad and strong frequency-dependent maximum dielectric permittivity. Moreover, the dielectric constant of relaxor ferroelectrics does not follow Curie-Weiss law. But, it can be described by quadratic Curie-Weiss law, as shown in Equation. (1.3)

$$\frac{1}{\epsilon} - \frac{1}{\epsilon_m} = \frac{(T - T_c)^\gamma}{C'} \quad (1.3)$$

Where  $T_m$  is the temperature at which  $\epsilon$  reaches a maximum,  $\epsilon_m$  is the value of  $\epsilon$  at  $T_m$ ,  $C'$  is the modified Curie Weiss like constant and  $\gamma$  is the critical exponent, explains the diffusivity of the materials, which lies in the range  $1 < \gamma < 2$  [68].

At the Curie point, the polarization decreases to zero relatively more rapid in ferroelectric materials compared to relaxor ferroelectric materials. The gradual decrease of the polarization in relaxors can be extended to the temperature above  $T_m$  and decays to zero at temperatures exceed  $T_m$ . At temperatures below  $T_m$ , relaxors can also show non-linear P-E behavior. However, the remnant polarization is much smaller than in normal ferroelectrics when the temperature is close to  $T_m$  as shown in Figure 1.4. Generally, these kinds of materials may undergo transitions between the following states. (i) When the temperature above  $T_m$ , the paraelectric (PE) state occurs, and (ii) upon cooling they gradually transform into an ergodic relaxor (ER) state with a random distribution of polar nano-regions (PNRs). Generally the transition temperature from PE to ER state is the so-called Burns temperature ( $T_B$ ) and is lower than  $T_m$ . It must not be confused with a structural transformations temperature since at  $T_B$  there is no macroscopic structure change. (iii) an intermediate non-ergodic state (true relaxor state) with short range ordered polar nano-regions appeared once the temperature is low enough. (iv) When a strong electric field is applied to the nonergodic state, the ferroelectric state appears. On the basis of ordered PNRs, the relaxor ferroelectric shows unique properties from dipolar glasses and normal ferroelectrics [69].

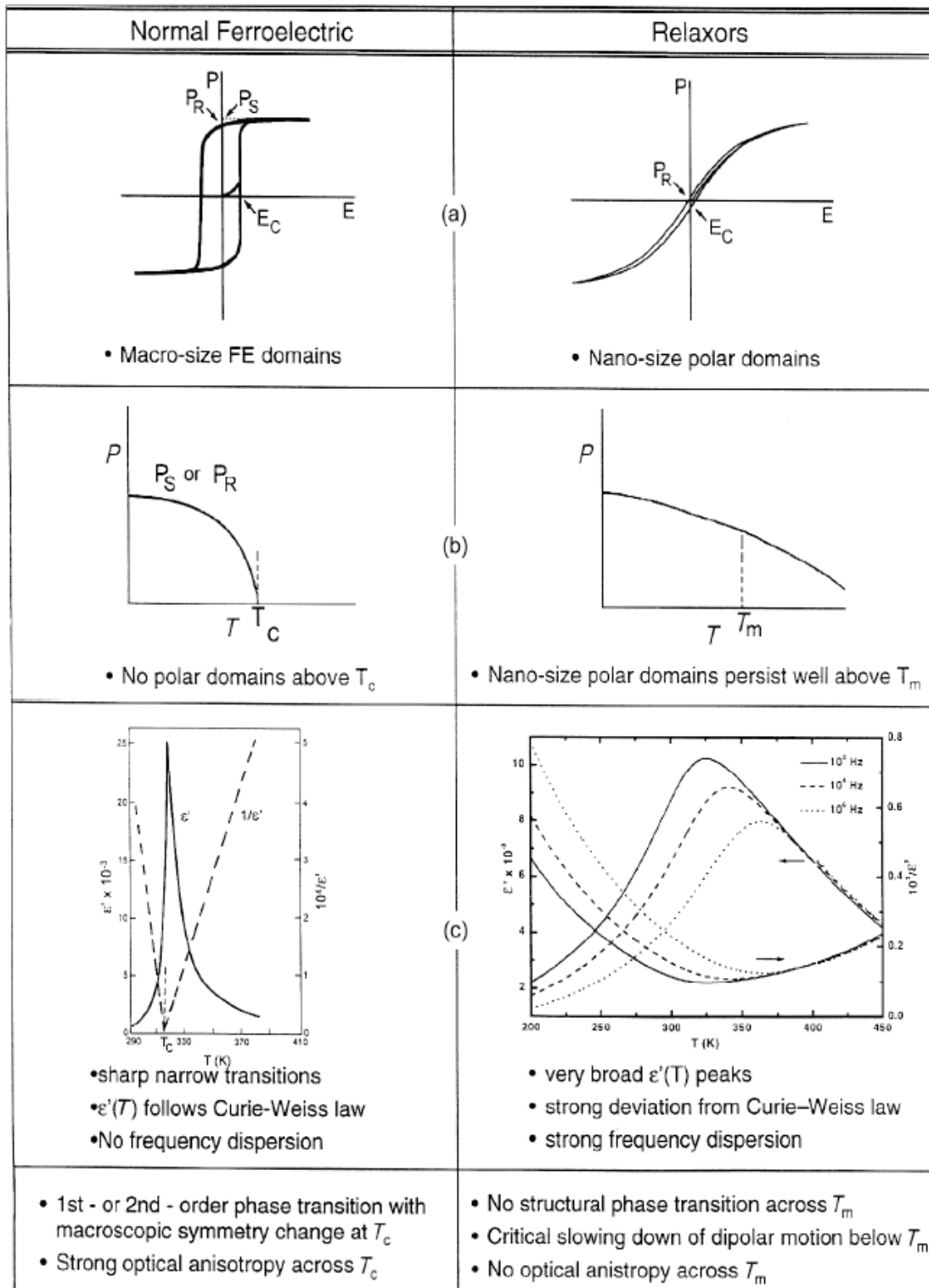


**Figure 1.4** Comparisons of normal ferroelectric and relaxor ferroelectric.

## 1.7 THEORETICAL MODEL TO EXPLAIN RELAXOR BEHAVIOUR

The relaxor behavior in normal ferroelectric materials results from a compositionally induced disorder or frustration. In the  $ABO_3$  perovskite oxides, substitution of ions of different sizes, valencies, electronegativities and polarizabilities at both A and B lattice sites produce dipolar defects and introduce a sufficiently higher degree of the disorder so as to break translational and prevent the formation of long-range order state [70]. In reflecting on the occurrence of relaxor behavior in perovskites, there appear to be three essentials ingredients: the existence of lattice disorder [71, 72], evidence for the existence of polar nanodomains at a temperature much higher than  $T_m$  and these domains existence as islands in highly polarizable (soft-mode) host lattice [73]. The existence of nano polar regions has also been evidenced by several other experimental techniques such as transmission electron microscopy [74], diffuse x-ray scattering and neutron diffraction studies [75]. A various physical model such as super paraelectric model, order-disorder transition model, microdomain and macro domain switching model, dipolar glass model and random field model has been proposed to explain the behavior of relaxor ferroelectrics (RFEs).

**Smolenskii (1959)**[76] proposed that the responsible factor for the relaxor behavior in  $PbMg_{1/3}Nb_{2/3}O_3$ (PMN) was compositional fluctuation due to the randomness in the B-site. The compositional fluctuation leads to the fluctuation in local field component, resulting in a distribution of transition temperature. This simple model has been widely cited, but it failed to explain the RFE behavior in the system without any compositional fluctuation.

**Burns and Dacol (1983)** [77] proposed that the polar regions (a region with net dipole moments) start appearing at a temperature much higher than  $T_m$  named as Burn temperature ( $T_B$ ). They have observed a deviation from the linear response refractive index with temperature, which



attributed to the nucleation of dipolar nano regions at  $T_B$ . The  $T_B$  was found to be very much close to the temperature at which the Curie-Weiss law begins to deviate. The dielectric behavior of REFs at a temperature lower than  $T_B$  is mainly dependent on the concentration and dipole moment of polar nano regions.

**Cross (1987)** [78] proposed in his super paraelectric model that the relaxors possess polar micro-regions that are dynamically disordered above  $T_m$ . The cation continuously flips between equivalent directions when activated by thermal energy. The heterogeneity caused by mixed B-sites creates locally favorable directions. Therefore, local symmetry is different from global symmetry. However, the energy barrier separating the different direction is so small that the polar domains do not extend to a larger size as in normal ferroelectrics. The relaxation mechanism involved in RFEs seems to be a deviation from Debye type.

**Viehland et al. (1990, 1991)**[79] proposed a glassy polarization behavior for RFEs and successfully explained the frequency dependence of  $T_m$  in 0.9PMN-0.1PT using the Vogel-Fulcher relation (V-F law). Later, many authors confirm that the polar clusters in the RFEs freeze at a low temperature similar to the dipolar glasses.

**Bell(1993)**,[80] explained the behavior based on ideal super paraelectric by considering an ensemble of independent, identical, nano-sized super paraelectric cluster, with distribution in the size of clusters. Taking the temperature dependence on cluster sizes and interactions into consideration, the calculation is carried out employing Landau-Ginsberg-Devonshire Formalism to determine the dielectric function of clusters.

**Glazounov et al. (1995)** [81] introduced the possibility of distribution of local transition temperature of the polar regions. The model considers the relaxors as an ensemble of non-interacting polar regions with unique size. It could explain the static polarization and the real part

of permittivity to some extent but fails to explain the imaginary part of permittivity and the relaxation time phenomena. This suggests that there exists a distribution of the size of the polar regions in RFESs.

**Lu and Calvarin (1995)** [82] assumed an exponential distribution of the size of the polar region. The model predicts that the dielectric absorption always increases with increasing frequency, which contradicts the experimental results in the low-temperature range.

**Cheng et al. (1998)** [83] proposed a power law to explain the relation between  $T_m$  and frequency. To explain the behavior of polar clusters, they have also proposed a model in which the relation between the frequency and dielectric constant at temperatures much lower and higher than  $T_m$  can be expressed by two exponential functions. The analysis at high temperature gives the information about the production rate and the concentration of polar cluster whereas the analysis at low-temperature range gives an idea about the freezing of polar clusters.

**Glazounov and Tagantsev (2000)**[84] proposed a phenomenological model, which describes frequency dispersion of nonlinear dielectric response of RFEs as a result of dispersion of their linear dielectric permittivity. It provided a good qualitative description of temperature and frequency dependence of the third harmonics of PMN.

**Kleemann (2006)**[85]reported that the substitutional charge disordered giving rise to quenched electric random- fields are probably the origin of the peculiar behavior of relaxor ferroelectrics. Spatial fluctuation of the RFs correlates the dipolar fluctuations and gives rise to polar nanoregions in the paraelectric regime evidenced by piezoresponse force microscopy at the nanoscale. The frustrated interaction between the polar nanoregions in the cubic relaxors provides rise to cluster glass states as evidenced by strong pressure dependence, typical dipolar

slowing- down and theoretically treated within a spherical random bond- RF model. On the other hand, freezing into a domain state takes place in uniaxial relaxors.

**Samara and Venturini (2006) [86]** reported the influence of hydrostatic pressure on the dielectric properties of compositionally disordered  $ABO_3$  perovskites had been the discovery of a pressure-induced FE to RFE crossover making the RFEs state, the ground state, of these materials at reduced volume. They have observed that the pressure favors the RFE state and biasing field's favors the FE state. The combined results provide new insights into physics and can be explained in terms of changes in correlation length for dipolar interaction among the nano-regions (PNRs) that exists in these disordered materials.

## **1.8 OBJECTIVES AND SCOPE OF PRESENT WORKS**

Lead-based perovskite oxides such as lead magnesium niobate  $PbMg_{1/3}Nb_{2/3}O_3$  (PMN) and lead iron niobate  $PbFe_{1/3}Nb_{2/3}O_3$  (PFN) exhibits relaxor behavior. The lead-based relaxor materials have two major drawbacks due to the presence of Pb: (i) volatility and (ii) toxicity. These drawbacks of lead-based relaxor materials prompted researchers to explore new relaxor materials. Towards this effort  $BaTiO_3$  based solid solutions were discovered as relaxor materials an alternative to Pb based relaxors. To achieve this goal extensive research works were carried out on solid solution  $BaTi_{1-x}Sn_xO_3$ .

Barium titanate stannate,  $Ba(Ti_{1-x}Sn_x)O_3$  is a binary solid solution system composed of ferroelectric barium titanate and non-ferroelectric barium stannate. This material system may find application for various purposes because the Curie temperature or dielectric constant of these types of system could be widely shifted by changing the wt% of tin in this scheme. The permittivity is very high as well as temperature is biased field sensitive. Therefore, it can be used

in various potential applications, such as a capacitor, bolometer, actuator [87, 88] and microwave phase shifter [89].

The performance of  $\text{BaTi}_{1-x}\text{Sn}_x\text{O}_3$  ceramics depends on the microstructure of the sintered body, which is influenced by characteristics of the starting powders. Therefore, attention has been focused on the synthesis of high-quality BTS nanopowders. Different chemical methods such as sol-gel [90], co-precipitation [91], low-temperature aqueous solution [92], low-temperature semi-wet [93], and combustion [94] have been used. These methods are not cost-effective for mass production of BTS powders for industrial applications. Thus, preparation of  $\text{BaTi}_{1-x}\text{Sn}_x\text{O}_3$  powders using solid-state reaction method is regarded as one of the most practical and economical ways because it does not require expensive chemicals as well as sophisticated equipment. This process is environment-friendly, and no toxic or unwanted waste is produced after the solid-state reaction is complete. This method is most suitable for mass production of BTS powder for industrial applications. In the conventional solid-state reaction method, BTS powders are usually produced via the reaction between the mechanically mixed  $\text{BaCO}_3$ ,  $\text{TiO}_2$  and  $\text{SnO}_2$  compounds by calcination at a temperature greater than or equal to  $1200\text{ }^\circ\text{C}$  [95]. Unfortunately, the reactions take place at such a high temperature beyond control that the resultant powders often have a large particle size and wide size distribution, etc. It is reported in the literature that formation of  $\text{BaTiO}_3$  and  $\text{BaSnO}_3$  can take place at a lower temperature ( $600\text{--}700\text{ }^\circ\text{C}$ ) when  $\text{BaCO}_3$  is replaced by  $\text{Ba}(\text{NO}_3)_2$  [96,97]. Based on the literature survey, following investigations have been carried out ;

1. Synthesis and characterization of a few compositions of  $\text{BaTi}_{1-x}\text{Sn}_x\text{O}_3$  ( $x=0.0,0.05,0.15, 0.30$  and  $0.40$  ) using raw materials  $\text{BaCO}_3$ ,  $\text{TiO}_2$  and  $\text{SnO}_2$  to confirm that the formation of  $\text{BaTi}_{1-x}\text{Sn}_x\text{O}_3$  using conventional solid solution method takes place at temperature  $\geq 1200^\circ\text{C}$ .

2. Synthesis and characterization of a few compositions of system  $\text{BaTi}_{1-x}\text{Sn}_x\text{O}_3$  ( $x=0.0, 0.10, 0.20, 0.30$  and  $0.40$ ) using  $\text{Ba}(\text{NO})_3$ ,  $\text{TiO}_2$  and  $\text{SnCl}_4 \cdot 5\text{H}_2\text{O}$  to lower calcination temperature and hence cost of the production.

3. Though system  $\text{BaTi}_{1-x}\text{Sn}_x\text{O}_3$  has wide range of applications, in order to further improve the properties of this system and hence broaden its applications, in this work we have tried to synthesize and characterize following composites also;

(i) BTS - NF -  $(1-x) \text{BaTi}_{0.85}\text{Sn}_{0.15}\text{O}_3$ -  $x\text{NiFe}_2\text{O}_4$  ( $x=5, 10, 15$  and  $20$  weight %)

(ii) BTS-CNT -  $(1-x) \text{BaTi}_{0.85}\text{Sn}_{0.15}\text{O}_3$ - $x\text{CNT}$  ( $x=5, 10, 15$  and  $20$  weight %)

(iii) BTS-Fly Ash -  $(1-x) \text{BaTi}_{0.85}\text{Sn}_{0.15}\text{O}_3$ - $x$  Fly Ash ( $x=5, 10, 15$  and  $20$  weight %)